



POLITECNICO
MILANO 1863

RE.PUBLIC@POLIMI

Research Publications at Politecnico di Milano

Post-Print

This is the accepted version of:

P. Gamba, E. Goldoni, P. Savazzi, P.G. Arpesi, C. Sopranzi, J.-F. Dufour, M. Lavagna
Wireless Passive Sensors for Remote Sensing of Temperature on Aerospace Platforms
IEEE Sensors Journal, Vol. 14, N. 11, 2014, p. 3883-3892
doi:10.1109/JSEN.2014.2353623

The final publication is available at <https://doi.org/10.1109/JSEN.2014.2353623>

Access to the published version may require subscription.

When citing this work, cite the original published paper.

© 2014 IEEE. Personal use of this material is permitted. Permission from IEEE must be obtained for all other uses, in any current or future media, including reprinting/republishing this material for advertising or promotional purposes, creating new collective works, for resale or redistribution to servers or lists, or reuse of any copyrighted component of this work in other works.

Permanent link to this version

<http://hdl.handle.net/11311/861145>

Wireless Passive Sensors for Remote Sensing of Temperature on Aerospace Platforms

Paolo Gamba, *Fellow, IEEE*, Emanuele Goldoni, *Member, IEEE*, Pietro Savazzi, *Member, IEEE*,
Pier Giorgio Arpesi, Claudia Sopranzi, Jean-François Dufour, and Michèle Lavagna.

Abstract—This work is devoted to the feasibility study of a wireless sensing system, mainly based on passive surface acoustic wave (SAW) sensors, for remote measurement of temperature aboard space platforms. The use of passive sensors is particularly attractive since they need no battery and are robust in extreme environments, as they contain no active electronic circuits. The main objective of this study is the complete characterization of the wireless system environment, in order to determine the main fundamental limits of this technology from a communication theory point of view. Preliminary experimental measurements are used for both defining the main environment parameters, validating some of the theoretical limit computations and proving the space application feasibility.

Index Terms—Wireless sensor networks, passive SAW sensors, space platforms.

I. INTRODUCTION

WIRELESS technology can be an important driver for enabling technology improvement of the near future space platforms and vehicles. Remote measurements of physical parameters can be collected by a wireless sensor network (WSN) for the ground testing campaign of aerospace platforms [1], with the future perspective of extension to on-board flight applications.

Thinking about both ground and in-flight operations, the wireless monitoring system must work in a very hostile environment [2]. The presence of metal cavities and obstacles makes the radio frequency (RF) propagation harder due to the multipath fading propagation channel, causing both line-of-sight (LOS) and non-line-of-sight (NLOS) radio communication conditions. Further, space conditions include operation under high vacuum and extreme temperature ranges with associated thermal stress and in presence of high levels of ionising radiations.

Sensors may be classified as active, passive or semi-passive depending on the fact they include or not active integrated

circuits and the way the energy is supplied to the sensor itself. In particular, active sensors are regarded as those devices that contain active integrated circuits (i.e. based on diodes and transistors) and the energy needed to supply these circuits comes from internal batteries on board the sensor.

Instead, truly passive sensors are defined as those sensors that do not contain any active circuit and therefore do not need any form of external energy supply other than the incoming signal itself. The energy comes from the interrogation signal and it does not power up anything but it is just backscattered with the physical parameter information. As far as semi-passive sensors are concerned, they may include active circuits but they do not contain batteries, as the required supply energy may be gathered either by harvesting techniques from the surrounding environment or directly from the RF interrogation signal after it has been duly rectified.

The above distinction is crucial in identifying the robustness of the sensors families, in fact the truly passive sensors are the most robust ones since they do not contain neither active circuits nor batteries. Active circuits are generally sensitive to temperature and ionizing radiation leading to a degraded reliability, batteries are very sensitive to temperature as well, which makes them critical items for space applications.

Although the use of active sensors may be suitable for the ground pre-launching testing campaign, passive or semi-passive sensors seem to be more feasible for in-flight operations, since they do not need batteries. For this reason, the main focus of this work will be on studying passive sensor applications. Indeed passive sensors represent an effective solution within hostile environments in virtue of their intrinsic ruggedness and reliability, which derive from their truly passive nature, as they have neither active circuits nor batteries inside. They also offer the option to be mounted on positions that are not easily accessible or hazardous, even on moving parts such as the panels of solar arrays when deploying after launch.

Surface acoustic wave (SAW) sensors could be the enabling technology for wireless space applications as they are passive, radiation-hardened, operable over wide temperature ranges, small, rugged, inexpensive, and identifiable [3] - [5].

A key aspect in system applications of SAW sensors is the ability for simultaneous multiple access, i.e. the avoidance of sensors collision [6], [7]. In fact, if a number N of sensors of the same type are placed within the field of view of a single interrogating antenna, there will be an interference produced by the $N - 1$ sensors with respect to the interrogated one. In a multi-sensor environment, it is necessary to both identify the

P. Gamba, E. Goldoni, and P. Savazzi are with the Department of Electrical, Computer and Biomedical Engineering, University of Pavia, Italy e-mail: givenname.surname@unipv.it.

P.G. Arpesi and C. Sopranzi are with Selex ES, Nerviano MI, Italy e-mail: piergiorgio.arpesi@selex-es.com, claudia.sopranzi@guests.selex-es.com.

J-F. Dufour is with ESA - ESTEC, European Space Technology Centre, 2200 AG Noordwijk, The Netherlands e-mail: Jean-Francois.Dufour@esa.int.

M. Lavagna is with Aerospace Science & Technology Dept., Politecnico di Milano e-mail: lavagna@aero.polimi.it.

An earlier version of this paper was presented at the IEEE International Conference on Wireless for Space and Extreme Environments (WiSEE 2013) and was published in its Proceedings: 10.1109/WiSEE.2013.6737567

Copyright (c) 2013 IEEE. Personal use of this material is permitted. However, permission to use this material for any other purposes must be obtained from the IEEE by sending a request to pubs-permissions@ieee.org.

sensor as well as to obtain the sensed information, then the SAW device becomes a tagged-sensor. Because SAW sensors are passive components without any active logic inside, they cannot be addressed individually if completely identical. To access simultaneously more than one sensor, specific techniques for multiple access are needed.

As a result, this work addresses -with an innovative approach- the use of the “wireless” option for sensing purposes on board space platforms. This is done by tailoring to the maximum possible extent the capabilities of the wireless sensing techniques on the specific application. A comprehensive technical background is provided first. On the one side, for the technical constraints relevant to the application, mainly consisting of the boundary conditions and the EMC requirements; on the other side, for the characteristics of the wireless sensors technologies. Then, preliminary analyses are performed to find out the guidelines for a sound architecture of the temperature measurement system as the best fit to the space application.

The paper is organized as follows: section II shows the operational environment and the wireless systems architecture definition. The subsequent section III is devoted to the description of the different techniques that can be used to discriminate several sensors connected to the same reader. Using the similarities with the well-known radio communication multiple access techniques, some analytic results about the configuration of the main communication system parameters are derived. Section IV presents the experimental measurements and the performance analysis of the reading process, based on system simulations. Finally, some concluding remarks about the wireless system analyzed and future research developments end this work. Some preliminary results of this work were presented in [2].

II. SYSTEM ARCHITECTURE

A. The Operational Environment

As shown in Fig. 1, the typical structure of a satellite system can be generally modeled as a set of separated and partially shielded cavities, which are enclosed by satellite panels, acting as metal walls. In addition a number of metallic boxes, i.e. the electronic equipment, are arranged within these cavities.

In order to provide a complete characterization of the wireless propagation channel within the actual scenario, it is important to specify the following aspects. The overall size of the metal cavities are on the order of a few meters, while the size of the internal units and equipment and the distances between them are of the order of tens of centimeters. All panels are metal type, so they represent a shield from an RF point of view. According to this description, the propagation channel can be modeled as both LOS and NLOS multipath fading.

Another important and crucial issue to take into account is related to the Electromagnetic Compatibility (EMC) specifications for space application. As reported in Fig. 2 and 3, both the radiated emission (RE) and the radiated susceptibility (RS) requirements represent strict and challenging specifications to be followed [8].

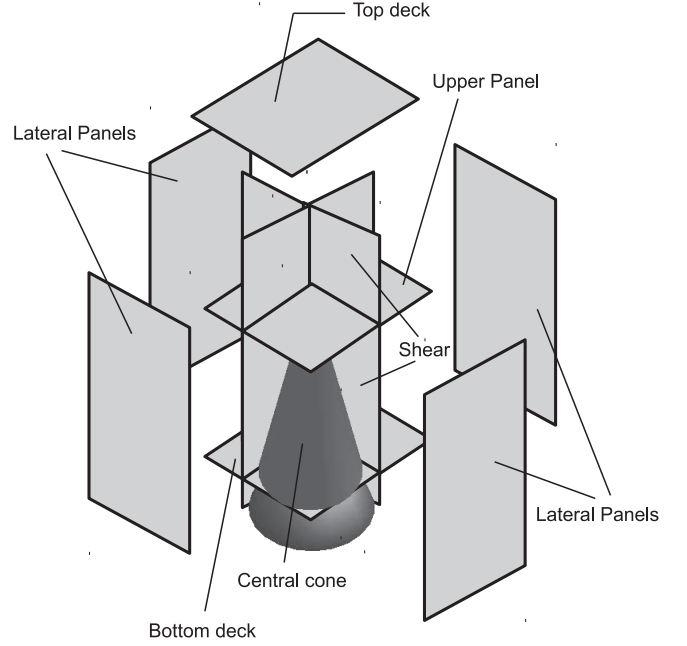


Fig. 1. Typical structure of a satellite as a composition of multiple cavities.

The frequency range (10 MHz to 1 GHz) shown in Fig. 2 and 3 is just a subset of the complete EMC standard specifications that generally cover the whole RF and microwave spectrum, from 50 kHz to 50 GHz. Indeed the presented limited range is the typical working frequency band of wireless sensing systems, where electromagnetic interference with the satellite electronic systems may occur.

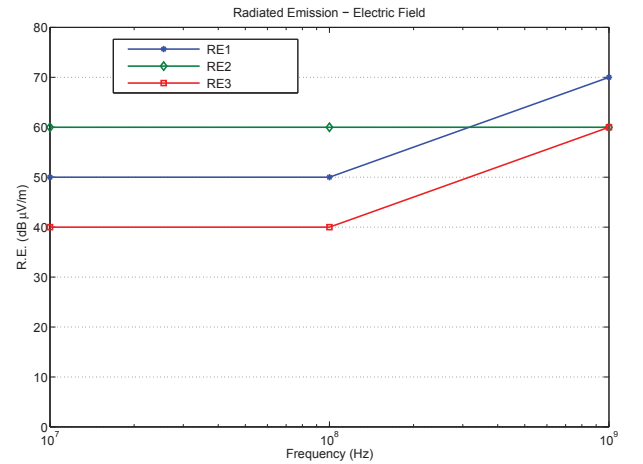


Fig. 2. Radiated emission requirements

In this paper we mainly focus on passive temperature sensors, limiting the analysis to the basic requirements given in table I, referring to the temperature range requested by most space applications.

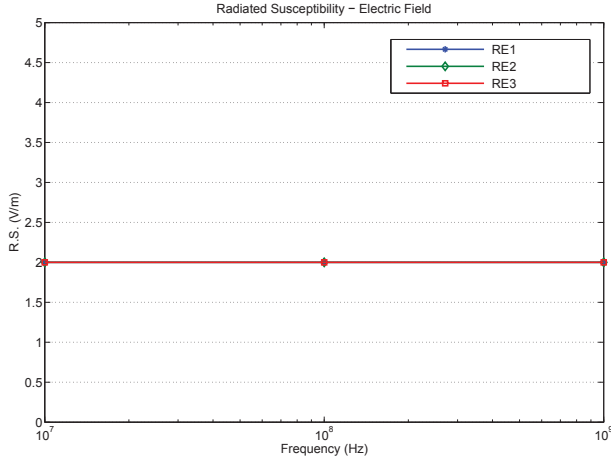


Fig. 3. Radiated susceptibility requirements

TABLE I
SENSOR TEMPERATURE SPECIFICATIONS

Range (°C)	$[-40, +90]$
Accuracy (°C)	± 2
Resolution (°C)	0.1
Maximum sampling time (s)	30
Maximum delivery measurement delay (s)	1

B. The Wireless Network System

The wireless network system architecture is described in Fig. 4, where its basic elements are:

- 1) sensor nodes, that can be based on active, passive or semi-passive technologies, according to the above definitions;
- 2) reader nodes, that interrogate one or more sensors and relay the information to the router nodes. It is a radio frequency receiver in case of active or semi-passive sensors, while it is a transceiver for the passive sensor case;
- 3) router nodes, which relay the information through the wireless network, in order to reach the main measurement interface for the ground testing case, or the platform system communication bus for the in-flight measurement acquisition.

Router nodes can be also used to relay the signal from one cavity to another, using propagation scattering.

Passive sensors present significant advantages in terms of both flexibility of placement and compatibility with moving parts. Moreover, they can be used in the most hostile environment conditions, since they do not need batteries and electronic chip.

For instance, in Fig. 5 the feasibility of using passive sensors for measurement of temperature of Satellite Solar Panels is shown. This also represents a typical on-board situation where the use of standard wired sensors has significant and very challenging constraints.

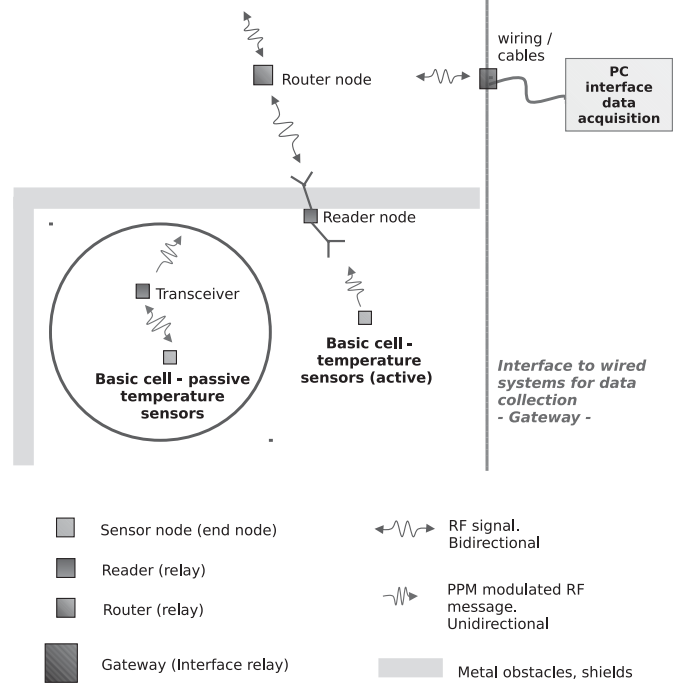


Fig. 4. System architecture

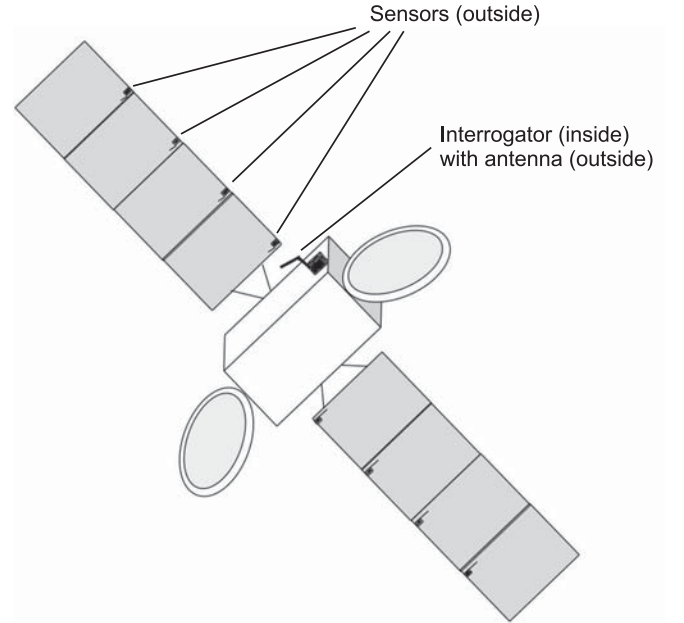


Fig. 5. Wireless Sensing Payload

C. SAW Passive Sensors

Sensing temperature with SAW devices is based on measuring the variations of the attenuation or velocity of acoustic propagation waves, due to the measured physical parameter changes.

A schematic layout of a SAW ID tag with several transducers wired together to a common bus bar is shown in Fig. 6. SAW devices are special components consisting of a

piezoelectric substrate with metallic structures such as inter digital transducers (IDTs) and reflection or coupling gratings deposited on its plain-polished surface [5].

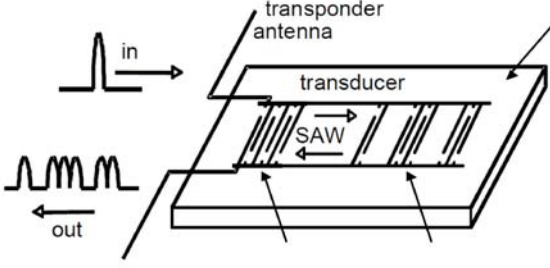


Fig. 6. Schematic drawing of a SAW ID tag

The remote interrogation of a wireless passive SAW sensor is carried out as in the following: the interrogation or reader unit generates a radio RF pulse at the sensor's center frequency. The pulse is converted into a surface acoustic wave on the sensor by a piezoelectric effect. The acoustic wave propagates along several reflectors on the sensor substrate.

Properties of the acoustic wave will be modified under the effect of the physical parameter which is sensed (e.g. temperature), thus a delayed pulse response signal is sent back to the readers antenna and processed to extract the temperature information.

Depending on the physical parameter which is sensed, the pulse velocity or its delay is modified. Thus we can measure:

- 1) the delay, or the corresponding phase;
- 2) the attenuation;
- 3) the frequency of the electrical response of the sensors.

III. MULTIPLE SENSOR DISCRIMINATION

One of the most critical aspect of implementing WSNs is the need of simultaneous interrogation of multiple sensors by the same reader, avoiding both interference and collisions [3], [4], [6]. The reader must be able to associate a unique tag to each sensor and the discrimination techniques can be derived from communication theory, according to the following classification: frequency division multiple access (FDMA), time division multiple access (TDMA), code division multiple access (CDMA), space division multiple access (SDMA), and different combinations of them [10] - [12].

A. FDMA

Sensor identification is pursued by assigning different resonance frequency responses to each tag. The resonance sensor frequency is determined by the distance between the reflector electrodes:

$$d = \frac{\lambda_{SAW}}{2} \quad (1)$$

The wavelength λ is related to the tag resonance frequency by $f\lambda = c_a$, where c_a is the acoustic propagation velocity on the tag. It is to be noted that the SAW storage time (delay) must

be longer than the duration of the decay of the environmental electromagnetic RF request echoes, in order to avoid collision with them. The storage time of the SAW component depends mainly on piezoelectric material and physical dimensions. The temperature measurement is achieved by detecting either the shift of the center frequency of the resonator or the variation of the time delay.

B. TDMA

Sensor identification relies on orthogonality in time, reflectors being located in different positions of the SAW physical length. It is worth noting that the satellite spacecraft application involves short distances, at most on the order of a few meters, thus around 10 ns propagation maximum delay for the RF signal is expected and this delay is far lower than the internal delays of the SAW device which are in the range 100 ns \sim 1 μ s as a minimum. For this reason no issue is envisaged due to spatial distribution of the sensors, and the relative positions of the sensors within the satellite environment is not relevant. However, the calibration of the system is needed after deployment of the sensors in their final positions.

C. CDMA

These multiple access schemes are generally based on spread spectrum (SS) techniques such as pseudo noise (PN) and orthogonal frequency coding (OFC), where N different sensors are distinguished basing on orthogonal codes. The bit impulse response $h_b(t)$, having a time length T , may be divided into an integer number of chips such that $T_b = NT_c$, where N is the number of chips. The chip impulse response for $j = 1, 2, \dots, N$, is:

$$h_{chip}^j(t) = a_j \text{rect} \left(\frac{t - jT_c}{T_c} \right) \quad (2)$$

for the PN coding case and:

$$h_{chip}^j(t) = a_j \cos(2\pi f_{0j}t) \text{rect} \left(\frac{t - jT_c}{T_c} \right) \quad (3)$$

for the PN-coded OFC case, where $f_{0j}T_b$ must be an integer, satisfying the orthogonality condition.

The bit impulse response can be then represented as in the following:

$$h_b(t) = \sum_{j=1}^N h_{chip}^j(t, f_{0j}) \quad (4)$$

According to the previous equations the maximum number of identifiable tags, without considering noise and interference, is:

- $N!$ for the OFC coding;
- 2^N for PN coding using perfectly orthogonal sequence;
- $2^N N!$ in case of OFC-PN coding

D. SDMA

This type of anti-collision approach is rather obvious as it is based on the re-use of the previously described systems in different metallic enclosures which have to be independent and isolated from an electromagnetic point of view. However, it is mentioned since it may be applicable to the satellite systems where multiple sections or cavities as above described can be identified within the satellite structure, both in the service module and in the payload. Each compartment should be within the same field of view of an interrogating antenna. The magnitude of the electromagnetic isolation between the cavities at the operation frequencies of the wireless system is paramount to establish whether the approach may work or not.

In the following, we compute some fundamental limits for the maximum number of identifiable tags, considering the multiple access gaussian channel [6], [9], [7].

E. Fundamental Limits

Although the theoretical analysis included in this paragraph is not completely related to the presented simulation and experimental results, we think that the provided information may help to understand the maximum reachable performance as well as the possible future system developments.

Let T be the time interval needed for both the transmission of an interrogator signal and the response receptions from all of the K tags in the environment. The returned signals have equal bandwidth B , and N_0 is the power spectral density of an additive white Gaussian noise (AWGN) source, the achievable capacity for each tag can be computed as [6]:

$$C = \frac{BT}{K} \log_2 \left(1 + \frac{K \text{SNR}}{BT} \right), \quad (5)$$

where $\text{SNR} = E_t/N_0$ is the signal-to-noise ratio, assumed to be equal for all the reader tags, and E_t represents the energy received for each tag.

C represents the maximum number of information bits communicated by each tag. The effective number of bits satisfies $R < C$. Further, equation (5) assumes that C is identical for all sensors.

The maximum number of identifiable sensors is given by the largest integer satisfying:

$$K \leq \frac{BT}{R} \log_2 \left(1 + \frac{K \text{SNR}}{BT} \right) \quad (6)$$

Equation (6) is very general and applies to all the discrimination techniques described above. Anyway, the actual number of discriminated sensors may be smaller due to the following reasons:

- equation (5) represents the maximum achievable capacity, i.e. the number of sensors to be discriminated without collisions, without considering hardware limits for the reader decoder complexity, and only for sufficiently large time-bandwidth products;
- the number of bits per tag $R < C$ does not include the supplementary bits needed for modulating the measured temperature information. Increasing the number of bits per tag means a larger time-bandwidth product.

It is interesting to note that one possible way to increase the time bandwidth product is given by the use of spread spectrum techniques.

F. WSN Capacity

Following the analysis described in [6], a more realistic expression for the system capacity and the maximum number of identifiable tags, considering a practical single-user detector, is defined as in the following:

$$R < C = BT \log_2 \left(1 + \frac{\text{SNR}}{BT + (K-1)\text{SNR}} \right) \quad (7)$$

$$K < \frac{2^{R/BT}}{2^{R/BT} - 1} - \frac{BT}{\text{SNR}} \quad (8)$$

Using equation (8) instead of (6) gives a more useful and realistic results.

Considering the satellite application faced in this work, we can define the following values for the system parameters:

- $R = 15$ bits, i.e. 10 bits are used for representing the measured temperature, while 5 bits are used for identifying a maximum of 32 tags;
- $B = 30$ MHz;
- $T = 10$ μ s;
- $\text{SNR} = 20$ dB.

The system is able to discriminate a maximum number of different sensors $K = 26$.

It is important to note that the available techniques to discriminate multiple sensors are based on random access protocols for semi-passive tags, while passive SAW tags must be discriminated at the receiver, if more than one tag falls within range of the reader

IV. EXPERIMENTAL RESULTS

In this section some simulation and experimental results are reported, showing the proposed solution feasibility for a system based on orthogonal frequency discrimination of multiple sensors. The two main aspects taken into account are the temperature measurement precision and the EMC test results.

A. Temperature Measurement Test

The validation of the wireless passive sensors technology for the remote temperature monitoring on board of space platforms has been performed through a thermal vacuum test campaign. For demonstrating the feasibility basing upon commercial wireless system, a Test Bed properly scaled to represent the space environment has been designed and implemented, as described in Fig. 7.

The CAD project has been developed by Politecnico di Milano with Selex technical support. The demonstrator includes the Thermal Vacuum chamber (the cylinder structure) which provides for the primary cavity, the baseplate adapter, the Palamede micro-satellite (acting as the secondary cavity) and Selex equipment units (TCU and ECM). The two rods (red color) on the TVAC side represent the two antennas for interrogating the sensors inside the TVAC chamber. The

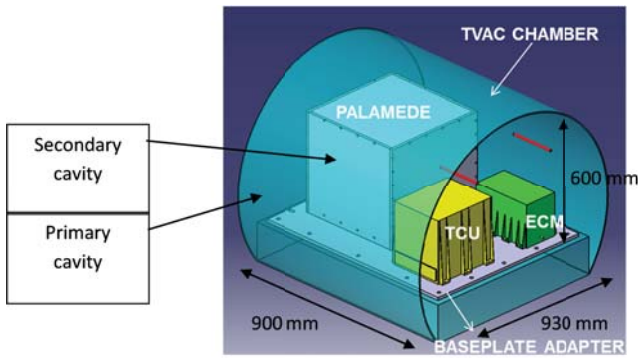


Fig. 7. Test bed assembly: 3D view CAD project

assembly of the test bed represents a typical configuration of a real satellite where the thermal vacuum chamber acts as a shielded cavity with sizes on the order of magnitude of 1 meter side cube. Palamedes envelope together with TCU and ECM reproduce the avionic units inside the satellite, as far as dimensions, materials and positioning between each other are concerned. The actual RF propagation aspects are also well represented:

- the test bed presents two different and partially shielded cavities both available for sensors placing, in order to verify Space Division Multiple Access (SDMA);
- the internally installed units (Palamede, TCU, ECM) are mainly composed of metal;
- LOS/NLOS conditions between sensors and relevant interrogating antennas are feasible due to the units geometrical location;
- mode stirred field distribution is expected.

Further, the demonstrator allows to reproduce a realistic temperature distribution over the required temperature range from -40°C to $+90^{\circ}\text{C}$.

Figures from 8 to 10 show the implemented test bed, highlighting the positions of the system elements in different open chamber views.

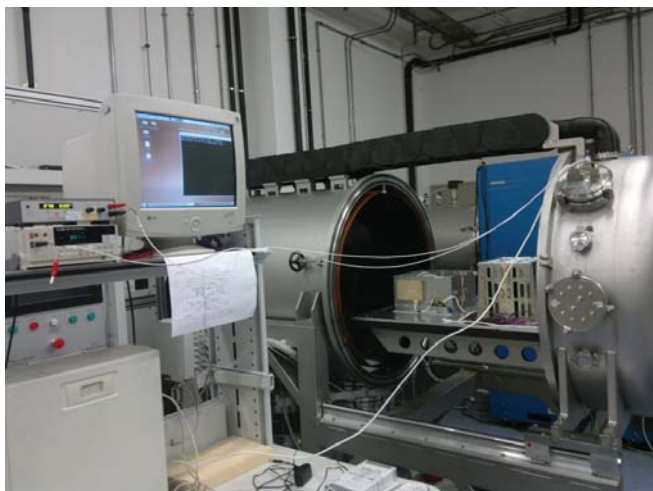


Fig. 8. Test bed implementation with TVAC

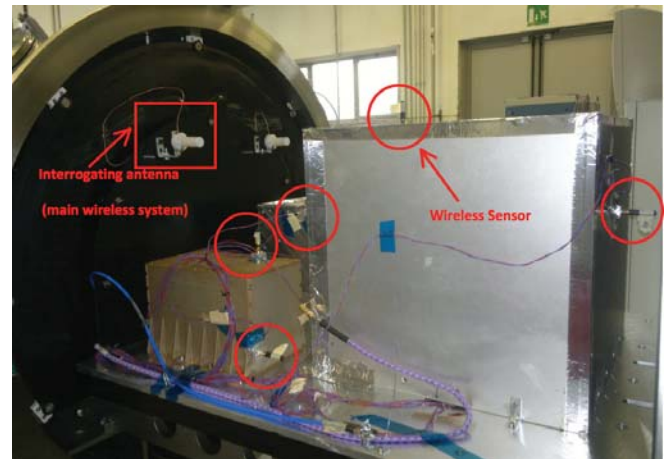


Fig. 9. Test bed implementation with TVAC: open chamber view

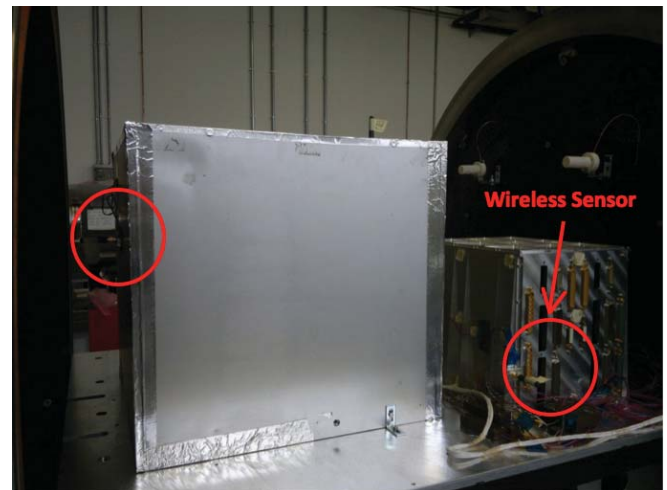


Fig. 10. Test bed implementation with TVAC: open chamber view

1) Test Campaign Results: The test campaign consisted in several temperature cycles in the range -40°C to $+90^{\circ}\text{C}$. Six wireless sensors were installed together with associated reference thermocouples for temperature reading comparison. Typical measurement results is reported in Fig. 11.

The temperature cycle duration is 18 hours with 1.5 hours for stabilization time at each temperature step. The temperature readings for the wireless sensor and the associated reference TC (thermocouple) are acquired with 1 s sampling time, after having duly synchronized the wireless system with the TC recorder. It can be observed that the responses of the wireless sensor and the thermocouple overlap precisely, providing for the accuracy indicated by the green curve. As a result, the observed accuracy, i.e. difference between wireless sensor and thermocouple (TC) readings, is generally better than 2°C as expected. It is also noted that the accuracy curve is peak-shaped due to the specific thermal time constant of the commercial wireless sensors which is greater than the TC time constant.

Moreover, since the subject sensing technology relies basically on RF communication, the system operation may be

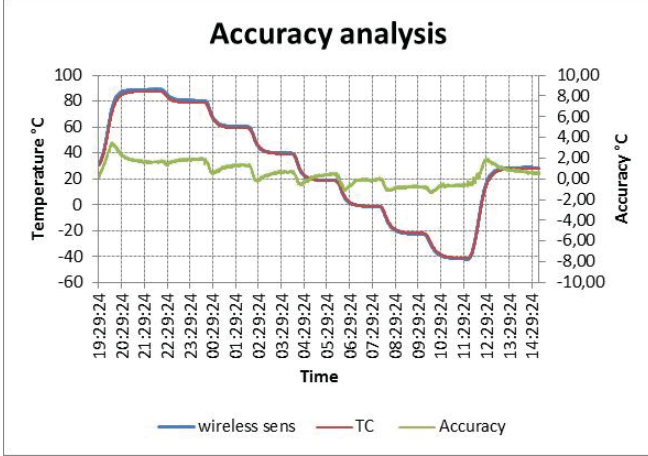


Fig. 11. Temperature measurement. Accuracy

affected by signal-to-noise ratio issues which may cause unexpected errors in temperature reading. Fig. 12 reports a typical temperature measurement where SNR issues were experienced leading to spikes in temperature detection. The root cause of the above behavior is more likely related to a sort of instability of the received signal, probably due to a mechanical/electrical instability of the specific wireless sensor when submitted to temperature cycling under high vacuum conditions. A further contributor could be also given by some anomalies of the Automatic Level Control (ALC) provision of the reader, that failed in power level controlling and a saturation effect was created as a consequence on the receiver.

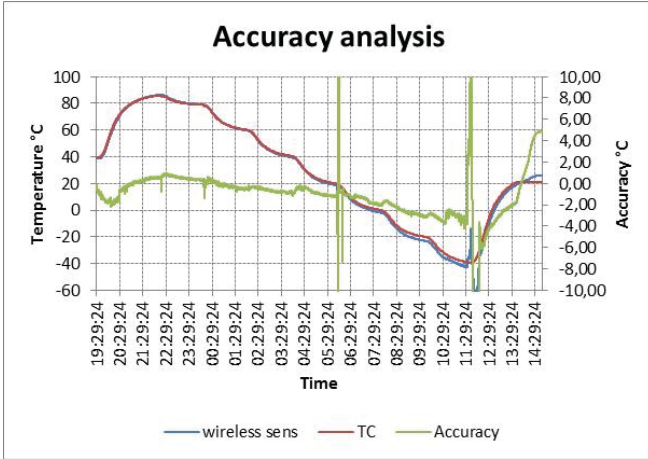


Fig. 12. Temperature measurement. Accuracy

2) *Simulation Performance Analysis:* In order to both validate and achieve a deeper understanding of the attainable performance, a behavioral model of the wireless sensor system has been realized, considering a scenario as close as possible to the test bed.

The simulated WSN system is composed of six sensors having the same features as the real system, AWGN noise, and variable channel attenuations to take into account the different physical positions of the SAW sensors inside the platform.

The channel attenuations have been randomly generated according to the Rayleigh distribution [10], considering the averages all equal to one. Actually, this setting represents a far worse case with respect to the real one, where the metal panel reflections tend to provide a uniform electromagnetic field distribution inside the cavities.

The main parameters used in the simulation runs are summarized in Table II.

TABLE II
SIMULATION PARAMETERS

Operating Frequency Range (MHz)	19
Sensor Bandwidth (MHz)	3
Number of Saw Sensors	6
Fractional Bandwidth	4%
Channel Attenuations (dB)	0.9, -6.4, -4, 1.8, -2.3, -3.1
SNR (dB)	20

Tables III and IV show the averaged accuracies and standard deviations obtained after 10^3 simulation runs, considering the channel attenuations given in Table II and temperatures generated randomly at each run, assuming a uniform distribution of the measured temperatures in the valid range (see Table I).

The largest value of accuracy standard deviation of the sensor 2 is due to the very high channel attenuation reported in Table II. This behaviour is similar to what is shown in Fig. 12 from experimental measurements. In this case the performance could be better with a lower fractional bandwidth which directly impacts on a greater energy consumption. The trade off between performance and energy saving must be considered with a particular care for the space-flight applications.

TABLE III
SENSOR ACCURACY AVERAGES

Sensor	Average Temperature errors (°C)
1	0.0204
2	0.0347
3	0.0233
4	-0.0061
5	0.0235
6	-0.0034

TABLE IV
SENSOR ACCURACY STANDARD DEVIATIONS

Sensor	Temperatures Standard Deviations (°C)
1	0.4226
2	10.1956
3	1.3314
4	0.3564
5	0.9172
6	1.0488

In the last three figures of this section, i.e. Fig. 13-15, the simulation runs have been generated considering the temper-

ature linearly varying from 90 °C to -40 °C, for the channel attenuations related to sensors 1,2 and 5 in Table II.

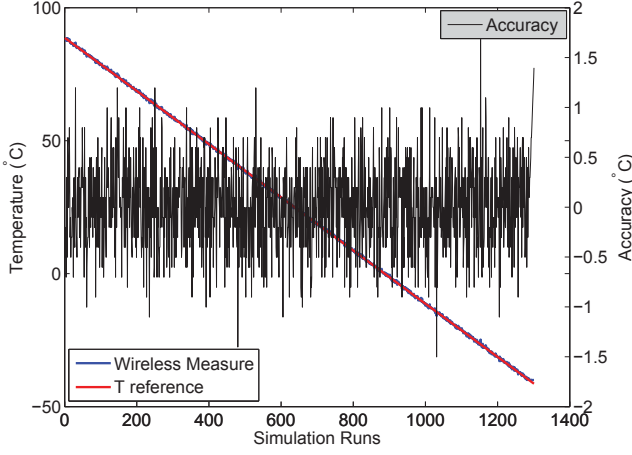


Fig. 13. Simulation Results for Sensor 1, with T varying from 90 °C to -40 °C

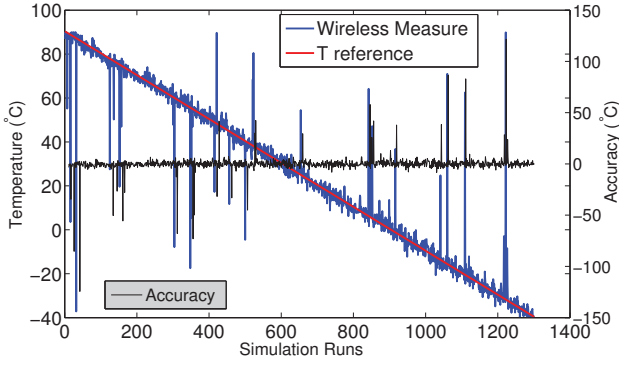


Fig. 14. Simulation Results for Sensor 2, with T varying from 90 °C to -40 °C

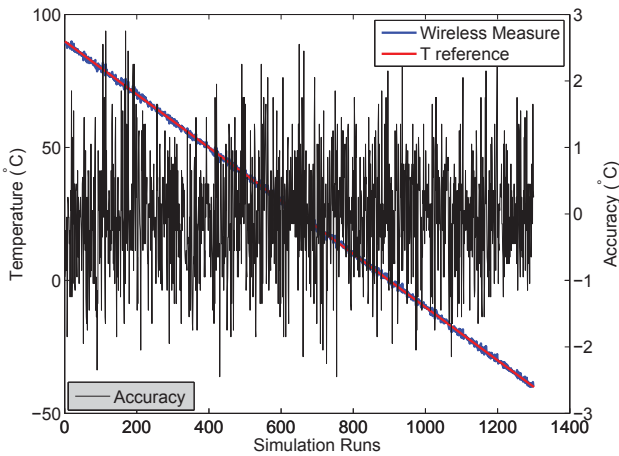


Fig. 15. Simulation Results for Sensor 5, with T varying from 90 °C to -40 °C

Simulation results look very similar to the experimental measurements of the previous subsection, especially for the channel attenuations closer to 0 dB.

B. EMC Test Results

The EMC verification has been carried out in terms of both radiated emission and susceptibility of a wireless passive system, by using a commercial off-the-shelf FDMA hardware with the following main operating characteristics: UHF band (around 430 MHz) with 10 dBm pulsed power level at interrogating antenna input.

It is underlined that the main contributor for the radiated emissions is represented by the interrogation signal since the echoes from the tags are negligible in this respect. Instead, as far as the radiated susceptibility is concerned, the tag response as received at reader side was considered in the test with respect to the interfering signal.

1) *Radiated Emission (RE), Electric Field*: The radiated emissions as measured within an anechoic chamber resulted in an electric field of 100dB μ V/m, i.e. 100 mV/m, at 1 m distance from the transmitting antenna, as shown in Fig. 16



Fig. 16. Test set-up for radiated emission

The emitted electric field of 100 dB μ V/m, see Figure 17, has to be compared with the 126 dB μ V/m (2V/m) tolerance generally required for the space equipments, that is 26 dB lower. As a conclusion, the wireless system seems not to be a disturbance to the on board electronic equipment.

2) *Radiated Scusceptibility (RS), Electric Field*: The test has been performed to verify the immunity of the DUT to the interference electric field. It has been verified that an Electric-field of 6mV/m (76dB μ V/m) is the threshold value beyond which the system does not work (this result is confirmed also by additional noise injection test performed within TVAC chamber). The test-setup is shown in Fig. 18.

Considering a 20 dB margin, 56 dB μ V/m is found as the limit for satellite emitted noise in order not to impact the wireless sensors system operation. Since about 10 dB are to be considered as the ratio between the RE value provided by equipment unit and the RE value at satellite level, 46 dB μ V/m

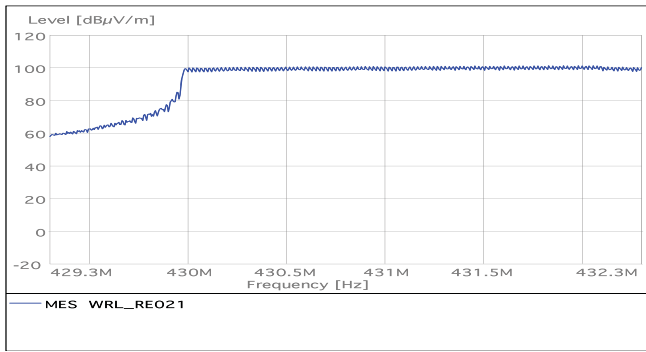


Fig. 17. RE measure. Operating Condition: 429.3-432.3 MHz.

is the limit for equipment noise. Considering that 60 dB μ V/m is the current RE requirement, a rejection notching of 14 dB at the system operating frequency (18 MHz bandwidth) should be defined and approved in the frame of the space committee.

This request seems absolutely feasible since the actual satellite noise as estimated from test data is typically around 40 dB μ V/m with the exception for some narrowband emissions which are up to 60 dB μ V/m. This analysis is generally valid for all mentioned interrogation schemes. However, it is worth underlining that those systems which rely on CDMA techniques show a lower emitted field, thanks to the spread spectrum modulation type.

The notching requirement for satellite RE has been relaxed with respect to what initially estimated in [2], after a detailed analysis of the complete test results.

V. CONCLUSION

Preliminary study results have been presented for the application of wireless sensing techniques on board space platforms, with particular regard to the passive sensors technology for remote measurement of temperature. This can be considered as the first step for the validation of Wireless Sensing Network technology for in-flight space applications. At first, a typical scenario for space operation is introduced together with the wireless system architecture, highlighting the advantages of using passive sensors in terms of flexibility, ruggedness and reliability. Then, a brief overview of the discrimination techniques for passive sensors ID-tags is given. The maximum achievable number of discriminated tags can be computed using fundamental results of communication and information theories. An interesting perspective of development could be the analysis of multipath fading, following a reasoning similar to those in [6]. Finally, test results on passive sensors systems available as commercial off-the-shelf are presented, mainly focusing on EMC aspects and temperature requirements compliance. Tests on EMC reveal that a wireless sensor system could operate within a spacecraft environment provided that a slight revision of the EMC Radiated Emission specification in terms of notching were approved at mission level. Furthermore, the wireless temperature sensors have been successfully operated in thermal vacuum chamber withstanding the environmental conditions typical of a spacecraft structure. An accuracy of $\pm 2^\circ\text{C}$ has been achieved over the required temperature range

-40°C $+90^\circ\text{C}$. In consideration of the growing interest for the wireless instrumentation from the major satellite integrators, it is expected that the wireless sensor technology will gain an increasingly important role disclosing for new potential applications in the space segment.

ACKNOWLEDGMENT

This work presents partial results of two parallel projects currently in progress: “Wireless Passive Sensors”, is funded by the European Space Agency (ESA) in the frame of the Innovation Triangle Initiative (ITI); the work of the authors from the University of Pavia was supported by the Italian Ministry of Education, University and Scientific Research under the project PRIN GreTa 2010WHY5PR.

REFERENCES

- [1] *Space Engineering - Testing*, ESA, ECSS-E-ST-10-03C. [Online]. Available: <http://www.ecss.nl/>
- [2] P. Gamba, E. Goldoni, P. Savazzi, P.G. Arpesi, C. Sopranzi, J-F. Dufour, “Wireless passive sensors for remote sensing of temperature on aerospace platforms,” in *Proc. IEEE International Conference on Wireless for Space and Extreme Environments (WiSEE)*, 2013, Baltimore, MD, USA, November 2013.
- [3] J. M. Pavlina, N. Kozlovski, B. Santos, and D. C. Malocha, “SAW RFID Spread Spectrum OFC and TDM Technology,” in *Proc. IEEE International Conference on RFID*, Orlando, FL, USA, April 2009.
- [4] J. M. Pavlina, and D.C. Malocha, “Chipless RFID SAW Sensor System-Level Simulator,” in *Proc. IEEE International Conference on RFID*, Orlando, FL, USA, April 2010.
- [5] L. Reindl, Member, G. Scholl, T. Ostertag, H. Scherr, U. Wol, F. Schmidt, “Theory and Application of Passive SAW Radio Transponders as Sensors,” *IEEE Transactions on Ultrasonics, Ferroelectrics, and Frequency Control*, vol. 45, no. 5, pp. 1281-1292, September 1998.
- [6] R.J. Barton, “Achievable Performance and Effective Interrogator Design for SAW RFID Sensor Tags,” in *Proc. IEEE Aerospace Conference*, Big Sky, MT, USA, March 2012.
- [7] R.J. Barton, “Some fundamental limits on SAW RFID tag information capacity and collision resolution,” in *Proc. IEEE International Conference on Wireless for Space and Extreme Environments (WiSEE)*, 2013, Baltimore, MD, USA, November 2013.
- [8] *Space Engineering - Electromagnetic compatibility*, ESA, CSS-E-ST-20-07C. [Online]. Available: <http://www.ecss.nl/>
- [9] T.M. Cover, J.A. Thomas, *Elements of Information Theory*. John Wiley & Sons, 2006.
- [10] J. G. Proakis, *Digital Communications*, 3rd ed. New York: McGraw-Hill, 1998.
- [11] A. Goldsmith, *Wireless Communications*. 3rd ed. Cambridge University Press, 2005.
- [12] T.S. Rappaport, *Wireless Communications: Principles and Practice*. 2nd ed. Prentice Hall, 2002.



Fig. 18. Test set-up for radiated susceptibility.